FULL PAPER

Estimating global geodetic parameters using SLR observations to Galileo, GLONASS, BeiDou, GPS, and QZSS

K. Sośnica*[ID], G. Bury, R. Zajdel, D. Strugarek, M. Drożdżewski and K. Kazmierski

Abstract

All Galileo, GLONASS, QZSS, and BeiDou satellites are equipped with laser retroreflector arrays dedicated to satellite laser ranging (SLR). Using SLR data to new GNSS systems allows for estimating global geodetic parameters, such as Earth rotation parameters, global scale, and geocenter coordinates. In this study, we evaluate the quality of global geodetic parameters estimated on a basis of SLR tracking of new GNSS satellites and the combined solution based on SLR observations to GNSS and LAGEOS. We show that along with a progressive populating of Galileo orbital planes, the quality of geocenter components based on SLR–GNSS data has been improved to the level of 6 and 15 mm for equatorial and polar geocenter components, respectively. The scale of the reference frame and the geocenter coordinates in the combined LAGEOS + GNSS solutions are dominated by the LAGEOS data. Some noncore SLR stations provide by far more observations to GNSS than to LAGEOS, e.g., Russian and Chinese stations dedicated to supporting GLONASS and BeiDou constellations. The number of solutions for these stations can be increased by up to 40%, whereas the station coordinate repeatability can be improved from about 20–30 mm to the level of 15–20 mm when considering both SLR to LAGEOS and SLR to GNSS.

Keywords: Satellite laser ranging, Multi-GNSS, Space geodesy, International Terrestrial Reference Frame, Geocenter, Earth orientation parameters

Introduction

Satellite laser ranging (SLR) is the space geodetic technique used for many applications (Pearlman et al. 2019), such as the realization of the origin and scale of the International Terrestrial Reference Frames (ITRF, Altamimi et al. 2016), determination of global geodetic parameters, such as polar motion and length-of-day (LOD) excess (Pavlis 1994; Sośnica et al. 2014; Glaser et al. 2015; Bloßfeld et al. 2018), determination of low-degree harmonics of the Earth's gravity potential (Cox and Chao 2002; Bloßfeld et al. 2015; Sośnica et al. 2015a; Cheng and Ries 2017), orbit determination and validation for active satellites and space debris (Arnold et al. 2018; Strugarek et al. 2019; Kucharski et al. 2017), time transfer (Exertier

et al. 2018), and verification of various general relativity effects (Ciufolini and Pavlis 2004; Pardini et al. 2017).

The SLR contribution to ITRF is based on observations to two LAGEOS satellites and two Etalons; however, the number of SLR observations to LAGEOS is more than ten times larger than that to Etalons (Appleby 1998). The contribution of Etalon to the ITRF realization is thus almost marginal. All new global navigation satellite systems (GNSS), such as GLONASS, Galileo, BeiDou, and Regional Navigation Satellite Systems, such as QZSS and NavIC, are equipped with laser retroreflector arrays dedicated to SLR tracking. Today, there are about 60 active GNSS satellites tracked by the International Laser Ranging Service (ILRS, Pearlman et al. 2002) stations. No active satellites, such as GNSS, are currently used for the ITRF realization, e.g., for the estimation of SLR station coordinates, geocenter coordinates, or Earth rotation parameters (ERPs). Some SLR stations, e.g., from the Russian SLR network, provide much more SLR observations

*Correspondence: krzysztof.sosnica@igig.up.wroc.pl
Institute of Geodesy and Geoinformatics, Wrocław University
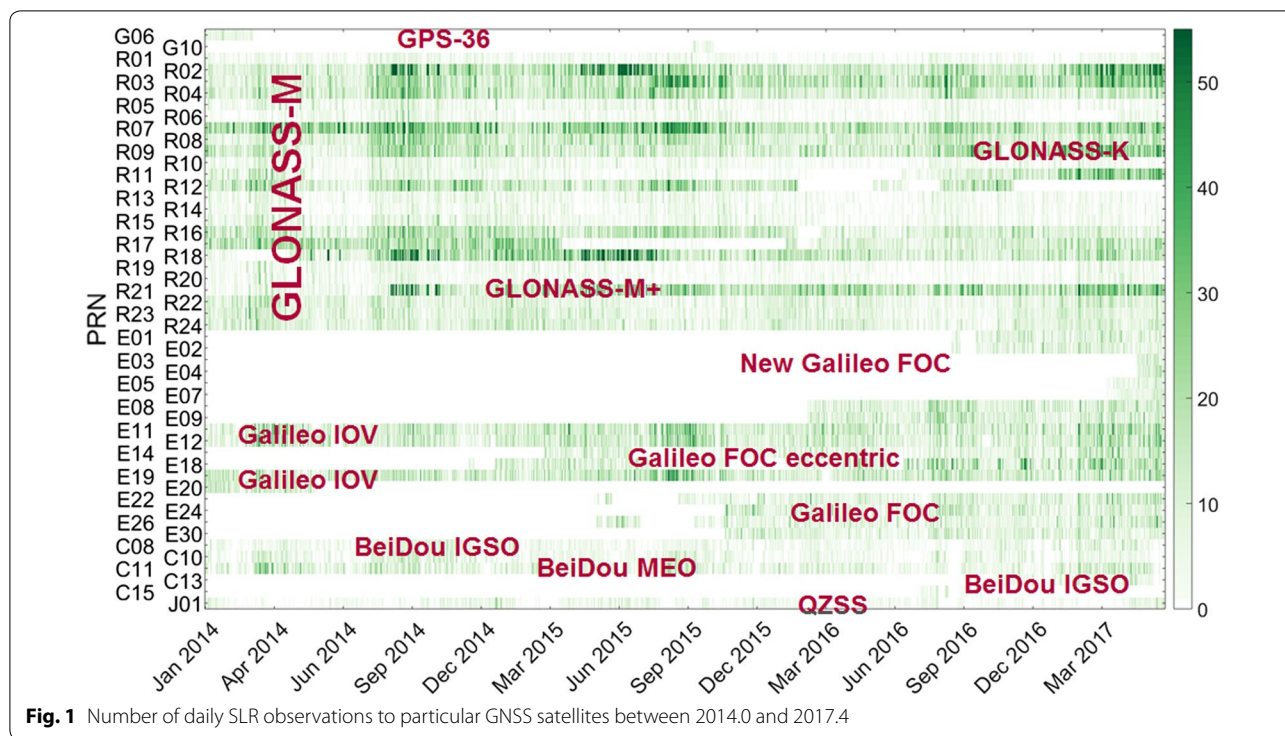of Environmental and Life Sciences, Grunwaldzka 53, Wrocław, Poland

Sośnica *et al. Earth, Planets and Space* (2019) 71:20

Page 2 of 11

Fig. 1 Number of daily SLR observations to particular GNSS satellites between 2014.0 and 2017.4

to GNSS than to LAGEOS, because these stations were dedicated to support the GLONASS system.

Between 2014 and 2017, the ILRS conducted a series of intensive campaigns tracking GNSS, which resulted in a substantial increase in the number of tracked GNSS spacecraft and the enlargement of the number of collected data. In this study, we use SLR observations to 1 GPS, 31 GLONASS, 18 Galileo, 1 BeiDou in medium Earth orbits (MEO), 3 BeiDou in inclined geosynchronous orbits (IGSO), and 1 QZSS satellite in inclined eccentric geosynchronous orbit (see Fig. 1). Not all spacecraft were active at the same time due to the constellation modernization, e.g., only up to 24 GLONASS were simultaneously active. In 2014, only 3–4 Galileo in-orbit validation (IOV) satellites were active. In 2017, the number of active Galileo increased to 17 due to multiple launches of Galileo fully operational capability (FOC) spacecraft (see Figs. 1, 2). A large number of SLR data allow, e.g., for the evaluation of geophysical effects using solely SLR observations to GNSS (Bury et al. 2019).

The performance of the combined solution based on LAGEOS and GNSS was assessed by Sośnica et al. (2018a). However, the results from the SLR-to-GNSS-only solutions have not been evaluated so far. In this study, we present results from the determination of global geodetic parameters associated with the ITRF realization, such as ERPs, geocenter, the global scale, and SLR station coordinates, based on both SLR observations to

GNSS and based on combined SLR-to-LAGEOS + GNSS data with different variants of handling satellite orbits and range biases.

Methodology

We estimate parameters with 7-day intervals: SLR station coordinates, geocenter coordinates, range biases, whereas ERPs are estimated with 1-day intervals and parameterized as piece-wise linear (see Table 1). In the case of LAGEOS solutions, range biases are estimated only for
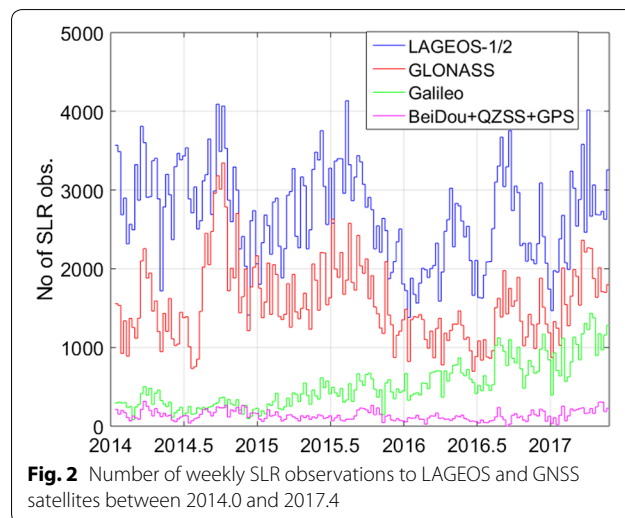

Fig. 2 Number of weekly SLR observations to LAGEOS and GNSS satellites between 2014.0 and 2017.4

Sośnica *et al. Earth, Planets and Space* (2019) 71:20

Page 3 of 11

Table 1 List of estimated parameters

Parameter	SLR@LAGEOS	SLR@GNSS
Common parameters		
Station coordinates	X, Y, Z for each station per 7 days with NNR/NNT constraints on core stations	
Pole coordinates	X pole, Y pole; eight parameters per 7 days using piece-wise linear parameterization	
UT1–UTC	Eight parameters per 7 days; fourth parameter fixed to IERS-14-C04	
Geocenter coordinates	X, Y, Z per 7 days	
Separate parameters		
LAGEOS orbits	6 Keplerian + 5 empirical:	–
	S_0, S_{S1}, S_{C1}, W_{S1}, W_{C1} per 7 days	
GNSS orbits	–	Fixed or estimated (see Table 2)
		6 Keplerian + 7 ECOM2
		D_0, Y_0, B_0, D_{S2}, D_{C2}, B_{S1}, B_{S1} per 5 days
Range biases	Selected stations; one value per 7 days	Depending on parameterization from Table 2

selected 1–2 sites following the recommendations of the ILRS Data Handling File.[1] We use the International Earth Rotation and Reference Systems Service series IERS-14-C04 (Bizouard et al. 2018) as the a priori ERPs and the ILRS realization of the ITRF2014, i.e., SLRF2014, for the a priori station coordinates. One UT1–UTC parameter is fixed to IERS-14-C04 series to provide absolute orientation of the network. For LAGEOS, we estimate six Keplerian orbit parameters and five empirical parameters, i.e., a constant acceleration, periodic once-per-revolution accelerations in along-track S and periodic accelerations in cross-track W with the 7-day intervals:

$$\begin{cases} R = - \\ S = S_0 + S_{S1} \sin u + S_{C1} \cos u \\ W = W_{S1} \sin u + W_{C1} \cos u \end{cases} \quad (1)$$

where u is the satellite argument of latitude. No empirical parameters are estimated in the radial direction R.

For GNSS, six Keplerian and seven empirical parameters are estimated of the new Empirical CODE Orbit Model (ECOM2, Arnold et al. 2015) with the expansion up to twice-per-revolution parameters in the satellite-Sun direction. In the empirical orbit model for GNSS, the estimated parameters are decomposed into three orthogonal directions: the D axis pointing from a satellite toward Sun, the Y axis lying along the solar panels, and the B axis completing the right-handed coordinate orthogonal frame. The set of estimated empirical orbit parameters for GNSS includes (Arnold et al. 2015):

$$\begin{cases} D = D_0 + D_{S2} \sin(2\Delta u) + D_{C2} \cos(2\Delta u) \\ Y = Y_0 \\ B = B_0 + B_{S1} \sin \Delta u + B_{C1} \cos \Delta u \end{cases} \quad (2)$$
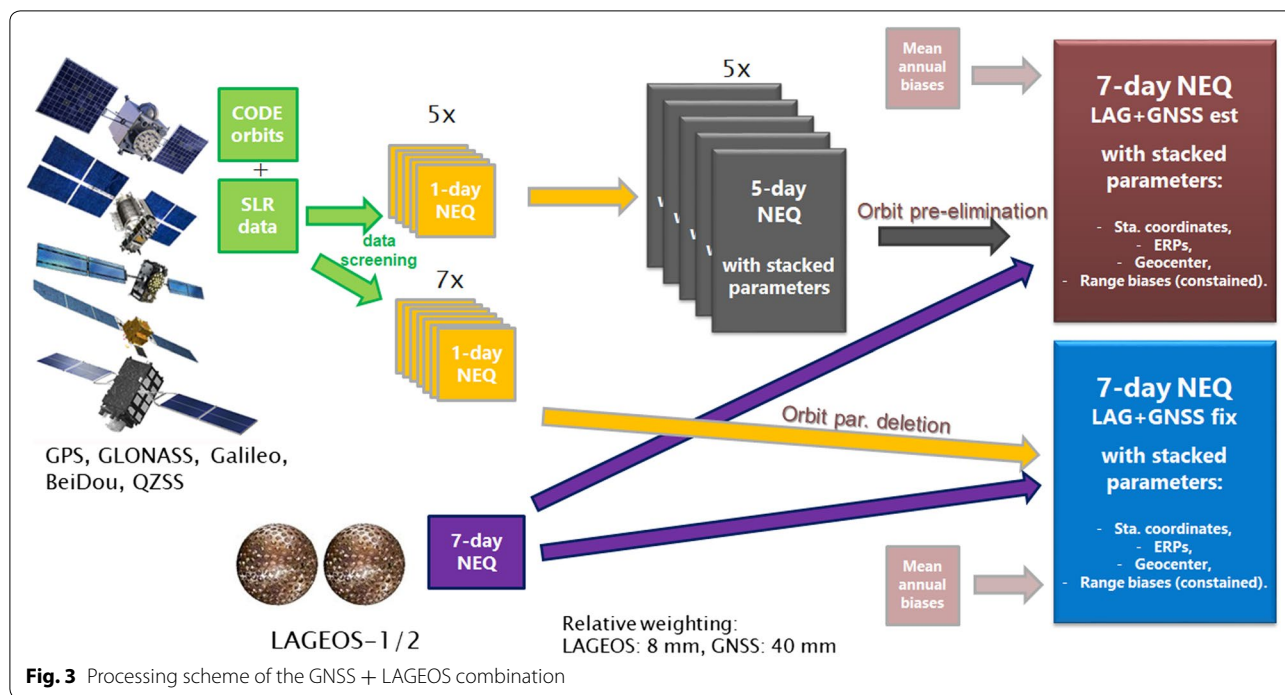
where Δu is the satellite argument of latitude with respect to the argument of latitude of the Sun. All orbit parameters are estimated without any constraints.

As a result, most of the parameters—SLR station coordinates, geocenter coordinates, ERPs—are common in the GNSS and LAGEOS solutions and can be stacked in the combination process. The only individually estimated parameters are range biases and satellite orbits (see Table 1).

We use the list of SLR core stations as recommended by the ILRS data handling file. The list of core stations is verified in every 7-day solution using the Helmert transformation. When the residuals after the 7-parameter Helmert transformation exceed the threshold of 25 mm for the north, east, or up component, the station is excluded from the list of core stations, and thus, the network constraints are not imposed thereon. Finally, we impose the no-net-rotation (NNR) and the no-net-translation (NNT) network minimum constraints using the verified list of core stations, whereas other station coordinates are estimated as free parameters.

We employ the same models for data reduction in the case of SLR observations to GNSS and to LAGEOS satellites. The Mendes and Pavlis (2004) model is used for the zenith path delay with a corresponding mapping function based on site-specific meteorological data. As the gravity potential model, we use EGM2008 (Pavlis et al. 2013) with a maximum expansion up to degree and order 30 and the ocean tide model FES2004 (Lyard et al. 2006). Solid Earth tides, pole tides, ocean pole tides, mean pole, ocean tidal loading displacements, and general relativistic corrections are modeled according to the IERS Conventions 2010 (Petit and Luzum 2010). The nontidal loading is here neglected, which may cause a systematic blue-sky effect up to 2 mm when fixing GNSS orbits (Bury et al.

---

[1] https://ilrs.dgfi.tum.de/fileadmin/data_handling/ILRS_Data_Handling_File.snx.

Sośnica *et al. Earth, Planets and Space*   (2019) 71:20

Page 4 of 11

Fig. 3 Processing scheme of the GNSS + LAGEOS combination

2019). The center-of-mass corrections for LAGEOS satellites[2] are applied as station and time dependent following the detector and detection procedure changes at individual SLR stations (Otsubo and Appleby 2003). For GNSS laser retroreflector offsets, we apply standard values provided by mission operators and distributed by the ILRS. We apply the time-variable retroreflector offsets with respect to the satellite center-of-mass for Galileo satellites,[3] which are caused by the fuel consumption. The time-variable offsets are, however, available only for Galileo.

We use the a priori multi-GNSS orbits provided by the Center for Orbit Determination in Europe (CODE, Prange et al. 2017). First, we generate 1-day normal equations (NEQs, see Fig. 3) based solely on SLR observations to GNSS in the Bernese GNSS Software (Dach et al. 2015). We stack five daily NEQs with the orbit transformations to continuous 5-day arcs because the 5-day arcs represent the optimum solution when using SLR data for the GNSS orbit determination (Bury et al. 2018). To allow a combination with the standard ILRS 7-day LAGEOS solutions, all solutions were transformed to the 7-day NEQs with the pre-elimination of all parameters exceeding the 7-day window and the pre-elimination of orbital

parameters before stacking. The pre-elimination guarantees that the parameters are estimated as implicit parameters, which means that their values cannot explicitly be estimated, but that all other parameters assume the values as in the case when all parameters were explicitly estimated (Dach et al. 2015). This procedure employing the 5-day orbit pre-elimination provides more stable parameters when compared to direct 1-day solutions based on sparse SLR observations to multiple satellites from the GNSS constellations. We generate also a second solution, in which the GNSS orbital parameters are not estimated; thus, they are directly fixed to the a priori CODE orbits.

Range biases constitute one of the major error sources when processing SLR data to GNSS (Thaller et al. 2014, 2015). Estimation of range biases substantially increases the number of estimated parameters when estimated as station-satellite specific. Therefore, we estimate first the mean annual station-satellite range biases and reintroduce them as a priori values in the final solution, in order to stabilize the solution and to reduce the number of estimated parameters. The estimated range biases absorb not only the station-specific biases and circuit delays, but also the satellite signature effects and the differences between detector types employed at the SLR stations (Otsubo et al. 2001; Sośnica et al. 2015b). Finally, we generate solutions with the contribution of LAGEOS satellites. We use the relative weighting of 8 mm for LAGEOS and 40 mm for GNSS, which is dictated by the quality

---

[2] https://ilrs.dgfi.tum.de/fileadmin/data_handling/com_lageos.txt.

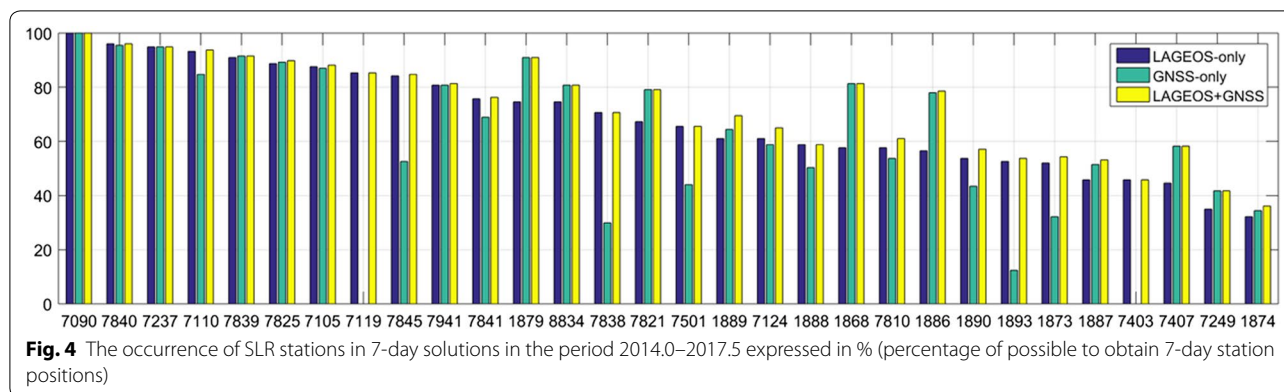[3] https://ilrs.cddis.eosdis.nasa.gov/missions/satellite_missions/current_missions/ga02_com.html.

Fig. 4 The occurrence of SLR stations in 7-day solutions in the period 2014.0–2017.5 expressed in % (percentage of possible to obtain 7-day station positions)

Table 2 Comparison of estimated ERPs to the IERS-14-C04 series

Solution			X pole (μas)		Y pole (μas)		LOD (μs)	
Sol.	Orbits	Bias	Mean	RMS	Mean	RMS	Mean	RMS
SLR to GNSS-only								
1	Estimated from SLR	Annual bias (sat & sta)	102	682	16	523	− 5	168
2	Fixed to a priori GNSS	Annual bias (sat & sta)	88	428	− 9	461	31	95
3	Fixed to a priori GNSS	Estimated every week (sat & sta)	72	617	38	520	− 1	87
4	Fixed to a priori GNSS	Estimated every week (sys & sta)	66	466	41	493	31	94
SLR to LAGEOS + GNSS								
5	LAGEOS-only	–	78	157	52	143	− 82	123
6	LAGEOS + GNSS (freely est.)	Annual bias (sat & sta)	82	154	55	143	26	69
7	LAGEOS + GNSS (fixed)	Annual bias (sat & sta)	74	149	51	141	1	43
8	LAGEOS + GNSS (fixed)	Estimated every week (sat & sta)	85	201	59	218	4	44

of the GNSS data from the SLR validation (Zajdel et al. 2017; Bruni et al. 2018).

Data

Figure 4 shows how many 7-day solutions in % are possible to obtain for particular SLR stations when using LAGEOS-only, GNSS-only, and LAGEOS + GNSS observations. In total, 177 weekly SLR solutions were generated in 2014.0–2017.4. The mean number of stations present in 7-day solutions is 22, 20, and 24 in LAGEOS-only, GNSS-only, and LAGEOS + GNSS, respectively. Some stations, such as Haleakala (Hawaii, station 7119) and Arequipa (Peru, 7403), do not observe GNSS satellites at all. However, most of the SLR stations observe LAGEOS and GNSS on the regular basis, e.g., Yarragadee (Australia, 7090), Herstmonceux (UK, 7840), Changchun (China, 7237), and Mt. Stromlo (Australia, 7825).
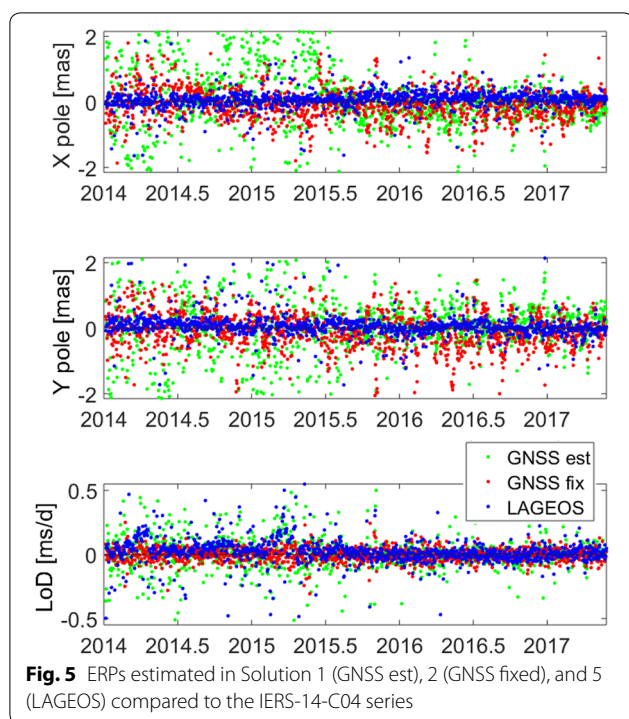
Some stations provide by far more observations to GNSS than to LAGEOS, e.g., for Altay (Russia, 1879) 132 weekly solutions were possible when using LAGEOS data and 161 solutions using LAGEOS + GNSS data (22%

more solutions), Komsomolsk (Russia, 1868)—41% more solutions, Arkhyz (Russia, 1886)—39% more solutions, Brasilia (Brazil, 7407)—30% more solutions. Other stations track both LAGEOS and GNSS, but provide more observations to GNSS, e.g., Beijing (China, 7249), Shanghai (China, 7821), Mendeleevo (Russia, 1874), and Wettzell (Germany, 7827). Most of these stations were build to support the GLONASS or BeiDou constellations by SLR tracking, time transfer, and GNSS clock synchronization using laser pulses (Meng et al. 2013); therefore, the GNSS targets have much higher priorities than the geodetic spherical satellites at those sites.

Results

SLR-to-GNSS-only solutions

We evaluate the quality of derived ERPs by comparing with the IERS-14-C04 series which is based on the combination of four space geodetic techniques: GNSS, SLR, very long baseline interferometry (VLBI), and Doppler Orbitography Radiopositioning Integrated by Satellite (DORIS). Four different GNSS-only solutions are generated (Solution 1–4, see Table 2): one solution with

Sośnica *et al. Earth, Planets and Space*   (2019) 71:20

Page 6 of 11

Fig. 5 ERPs estimated in Solution 1 (GNSS est), 2 (GNSS fixed), and 5 (LAGEOS) compared to the IERS-14-C04 series

the estimation of GNSS orbits based solely on SLR data (Solution 1), and three solutions with fixing the orbits to a priori CODE microwave-based solutions (Solutions 2–4). In Solutions 1 and 2, the range biases are fixed to the mean annual values estimated for every station-satellite pair. In Solution 3 and 4, the range biases are estimated as free parameters for every 7-day solution for every station-satellite pair (Solution 3) and for every system-satellite pair, i.e., one common value for all GLO-NASS satellites, all Galileo, etc. (Solution 4). We emphasize here that 'range biases' at the ranging stations refer both to 'true' instrumentation-based systematic effects plus effects induced by the large retroreflector arrays on the GNSS satellites.

Table 2 and Fig. 5 show that the largest RMS of pole coordinates of about 500–700 µas is obtained for the solution in which the GNSS orbits are estimated on the basis of SLR data (Solution 1). The value of 600 µas corresponds to 20 mm on the Earth's surface which is consistent with the quality of GNSS orbits derived from SLR data (Bury et al. 2018). The solution can be stabilized by fixing the GNSS orbits to microwave-based values (Solutions 2–4); however, when the biases are estimated every week as satellite-station-specific values (Solution 3), the RMSs of pole coordinates are similar to those from Solution 1. The ERP estimates can be stabilized through the re-substitution of mean annual range biases (Solution 2) or by reducing the number of estimated range biases by estimating system-specific values (Solution 4). However,
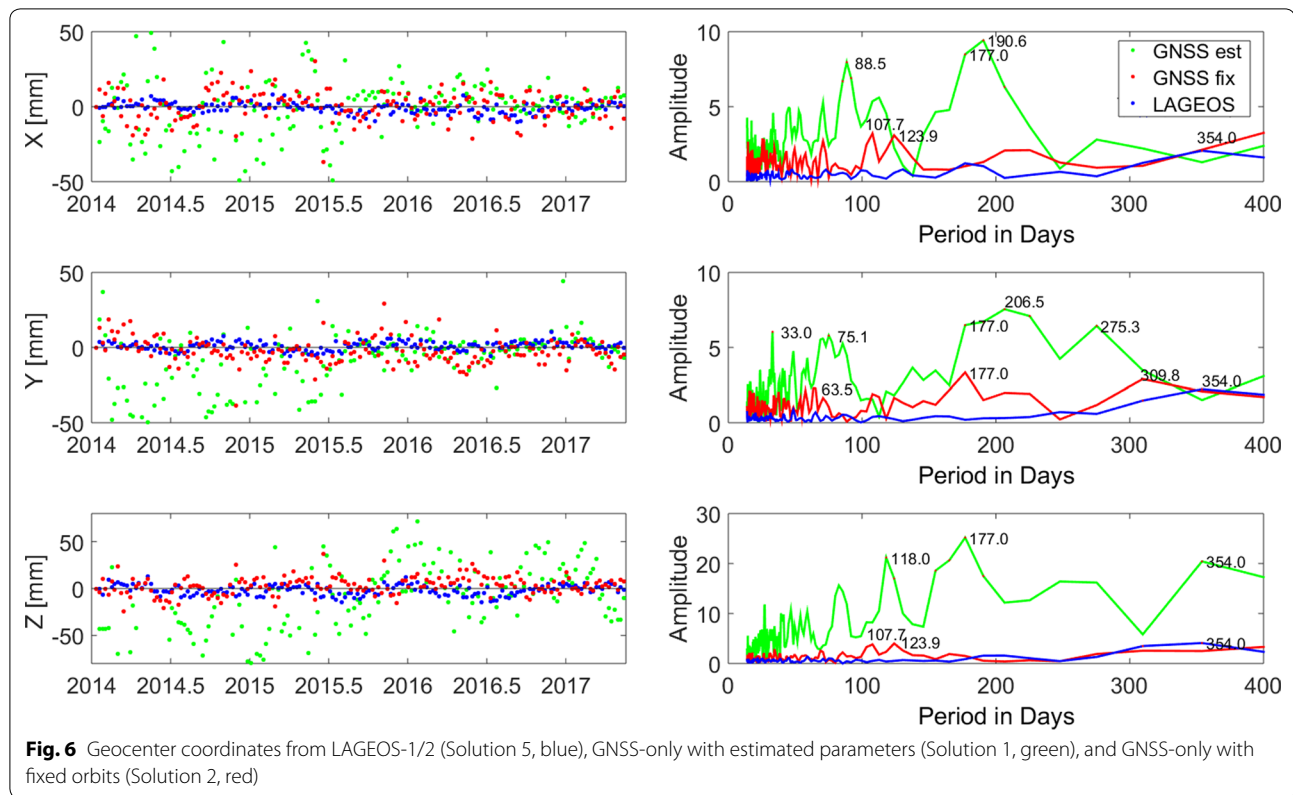
some satellites show different performance, such as mis-behaving GLONASS satellites in the plane #2 when compared to other GLONASS (Prange et al. 2017) or BeiDou IGSO and BeiDou MEO. Therefore, estimating one bias for the entire system may not properly account for all satellite-specific errors.

Figure 6 shows the geocenter coordinates derived from two GNSS-only solutions 1 and 2 as well as the LAGEOS-only solution (Solution 5). When fixing the GNSS orbits to the a priori values, the solution is stable, because the origin of the network is provided by the GNSS reference frame IGS14 with the accuracy of observation sensitivity to the reference frame origin and the orbit modeling accuracy. The satellite orbits are integrated around the IGS14 origin, which is fixed; thus, Solution 1 cannot realize a fully independent reference frame origin.

Solutions 2–4 realize the reference origin through the determined GNSS orbits and the ground network. Until 2016, the GNSS-only solution is strongly dominated by GLONASS, because all 24 GLONASS satellites were active at that time and provided about 90% of all observations (see Fig. 2). The geocenter coordinates derived by GLONASS-only are known to be affected by substantial orbit errors (Fritsche et al. 2014; Arnold et al. 2015; Lutz et al. 2016). The spectral analysis of the geocenter coordinates shows harmonics corresponding to the draconitic year of GLONASS (and other GNSS satellites, see Fig. 6, right): first harmonic (353 days), second harmonic (177 days), third harmonic (118 days), fourth harmonic (88 days), etc., which indicate serious GLONASS orbit modeling deficiencies when based on SLR data only. The draconitic signals have the amplitudes up to 26 mm and 4 mm for the Z geocenter component in Solution 1 and Solution 2, respectively, and up to 9 mm and 3 mm for the equatorial components. Recently, serious orbit modeling issues for GLONASS satellites especially from the second orbital plane have been discovered (Dach et al. 2017; Prange et al. 2017) which are caused by malfunctioning of transmitter antenna panels or problems with proper maintenance of the yaw satellite orientation.

In the beginning of 2015, only three Galileo IOV satellites were active. In 2015, two Galileo satellites launched into incorrect eccentric orbits were activated (Sośnica et al. 2018b) and six additional FOC satellites were launched into three additional Galileo orbital planes, which resulted in a population of all Galileo planes by FOC satellites by the end of 2015.

The number of active Galileo satellites reached 17 in 2017, and the number of SLR observations to Galileo increased from about 240 observations per week in 2014 to 1150 observations in 2017. In 2014, Galileo constituted only 10% of all SLR-to-GNSS observations, whereas in mid-2017 the percentage of Galileo observations

Sośnica *et al. Earth, Planets and Space* (2019) 71:20

Page 7 of 11

Fig. 6 Geocenter coordinates from LAGEOS-1/2 (Solution 5, blue), GNSS-only with estimated parameters (Solution 1, green), and GNSS-only with fixed orbits (Solution 2, red)

increased to 40%. Figure 6 shows the increasing contribution of Galileo satellites to the stabilization of GNSS-derived geocenter provided by SLR observations. Similar effect of the increasing contribution of Galileo on the quality of estimated pole coordinates and LOD is visible in Fig. 5, specially for the *X*-pole coordinate. The spectral analysis shows that in the solution with estimating GNSS orbits, the geocenter coordinates are strongly contaminated by orbit modeling issues, especially related to fewer observation opportunities in early years. However, starting from 2016, the geocenter coordinates can be derived from GNSS with the RMS of about 6 mm for the equatorial components and 15 mm for the Z component. In 2014, the stable geocenter and ERP solution with estimation of GNSS orbits (Solution 1) could be obtained only during the first ILRS intensive tracking, which took place in August–September 2015 and substantially increased the number of collected data (cf. Figs. 2, 6).

SLR-to-LAGEOS + GNSS solutions
LAGEOS-only solutions deliver the pole coordinates with the RMS of about 140–150 μas, corresponding to 5 mm on the Earth's surface and the RMS of 120 μs for LOD corresponding to 60 mm on the equator. When adding the SLR observations to GNSS (see Table 2), there is no significant improvement for the *X*- and

Y-pole coordinates, because in both solutions the NNR constraint is imposed on the same set of core SLR stations, whose station coordinates improve only slightly by adding GNSS data.

The combined GNSS + LAGEOS Solution 6 with the estimation of GNSS orbits is strongly dominated by the LAGEOS observations because of the much lower number of estimated parameters in the case of LAGEOS and larger weights imposed on LAGEOS observations. For LAGEOS-only, 11 orbit parameters have to be estimated per 7 days, whereas for GNSS, 13 parameters are estimated for each satellite and each 5-day arc, which substantially increases the number of parameters. The a priori sigmas between LAGEOS observations and GNSS are $\sigma_L:\sigma_G = 8{:}40$ mm, which corresponds to the ratio of weights $1/\sigma_L^2{:}1/\sigma_G^2 = 25{:}1$. We tested other sigma ratios between the LAGEOS and GNSS observations; however, increasing the GNSS weights always deteriorated the combination. Similar issues with inferior observation quality when compared to LAGEOS and issues with precise orbit determination are known for Etalon-1/2 which orbit at similar altitudes as GNSS satellites do. In this study, we use 55 satellites at the Etalon heights instead of two passive cannonballs used for operational ILRS products. Similar processing issues remain; however, GNSS satellites

are active satellites; thus, the microwave-based orbits can support the solution.

Solution 7 shows a similar quality of pole coordinates to the LAGEOS-only solution (Solution 5) and LAGEOS + GNSS solution (Solution 6). However, the LOD estimates can remarkably be improved when fixing the GNSS orbits to microwave-based values (Solutions 7 and 8) due to the reduction in the correlations between LOD and C_{20} from LAGEOS-only solutions when using the piece-wise-linear ERP parameterization (Bloßfeld et al. 2014). The RMS of LOD is reduced to 40 μs which corresponds to about 20 mm on the equator. Including GNSS satellites to the LAGEOS solutions reduces the RMS of LOD from 123 to 69 μs from Solution 5 to 6, respectively, whereas fixing GNSS orbits to microwave-based values reduces the LOD bias with respect to IERS-14-C04 series from 26 to 1 μs.

Including the estimation of range biases on the weekly basis substantially increases the number of estimated parameters and thus destabilizes the estimates of pole coordinates to the level of 200 μas (cf. Solution 7 and 8). Therefore, estimating one bias per satellite and station for a longtime span, e.g., 1 year, and re-substituting the bias as a priori known quantity reduced the impact of systematic effects, such as the detector-specific signature effect. A similar approach with estimating long-term mean biases and re-substituting them for LAGEOS and Etalon satellites will be employed by the ILRS Analysis Standing Committee after the completion of the dedicated Pilot Project 'Determination of Systematic Errors in ILRS Observations.'[4]

ERPs describe the orientation between the ground network realized by stations and the inertial frame realized by artificial satellites. We can thus conclude that SLR observations to GNSS allow for the transfer of the network orientation from GNSS to SLR solutions with the accuracy of about 15 mm.

Figure 7 shows the examples of two SLR stations decomposed into the up, north, and east components for Baikonur (Kazakhstan, 1887) and Wettzell (Germany, 8834) from Solutions 5, 6, and 7. When both LAGEOS and GNSS observations are available, the solution is dominated by LAGEOS data. Starting from the beginning of 2017, Baikonur started providing a very low number of SLR observations to LAGEOS; thus, for most of the weeks, the LAGEOS-only solution was not possible at all. However, when considering SLR observation to GNSS, the regular weekly solutions can be generated with the similar quality of the LAGEOS solution especially in the
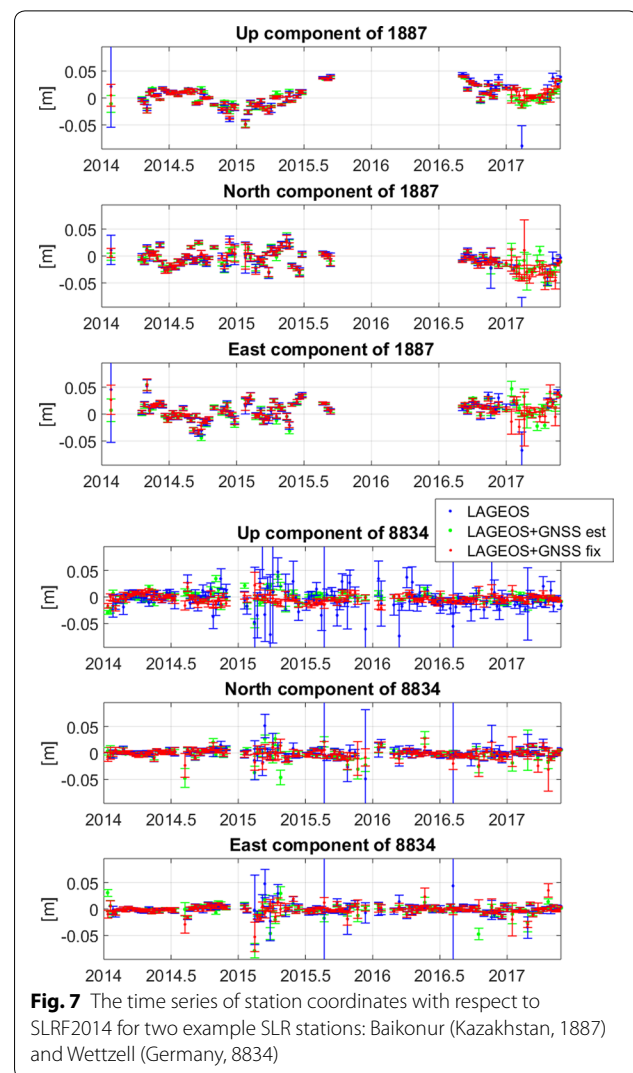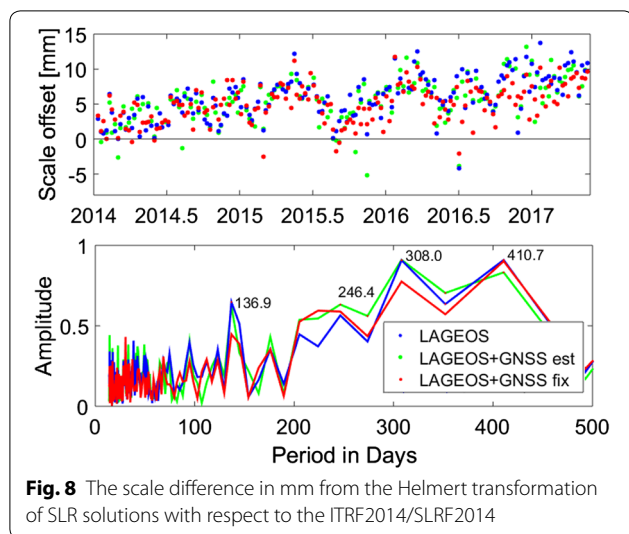
Fig. 7 The time series of station coordinates with respect to SLRF2014 for two example SLR stations: Baikonur (Kazakhstan, 1887) and Wettzell (Germany, 8834)

case of Solution 7 when fixing GNSS orbits. The GNSS solution with fixing orbits is similar to that when using both SLR and microwave observations in one combined solution.

Range biases are estimated for Wettzell in the case of LAGEOS solutions. The estimated biases are strongly correlated with the vertical station component which leads to the noisier 'Up' component for the LAGEOS-only solution shown in Fig. 7. Adding the SLR observations to GNSS allows for a better decorrelation between estimated LAGEOS range biases and the station coordinates and stabilizes the solution characterized by the station coordinate repeatability at the level of 25 mm in LAGEOS-only to the level of 7 mm in the combined LAGEOS + GNSS solution with fixed GNSS orbits. Moreover, the number of weekly solutions for Wettzell is increased from 132 to 143 solutions, which means that about 8% of solutions are based on GNSS-only data.

Sośnica *et al. Earth, Planets and Space* (2019) 71:20

Page 9 of 11

Fig. 8 The scale difference in mm from the Helmert transformation of SLR solutions with respect to the ITRF2014/SLRF2014

SLR and VLBI techniques are used for the scale realization in ITRF. In ITRF2014, the scale discrepancy between the two techniques is at the level of 7–8 mm, which constitutes currently a subject of discussions and investigations in both the SLR and VLBI scientific communities (Bachmann et al. 2016; Appleby et al. 2016). In this solution, the mean scale offset and standard deviations equal 6.1 ± 3.1 mm, 5.7 ± 3.2 mm, and 5.2 ± 2.7 mm in LAGEOS-1/2 (Solution 5), LAGEOS + GNSS (Solution 6), and LAGEOS + GNSS with fixed orbits (Solution 7), respectively. The scale offset is thus only slightly reduced when adding GNSS to LAGEOS observations; however, the scatter of the scale is reduced from 3.14 to 2.71 mm (see Fig. 8). An improvement in the scale offset is not expected when adding SLR observations to GNSS, as the scale strongly depends on the handling of range biases. We generated the spectral analysis of all three scale series, which did not show any significant differences (see Fig. 8). No differences mean that the scale is mostly dominated by LAGEOS observations and not affected by GNSS solutions, which typically are contaminated by draconitic periods. The dominating periods are related to LAGEOS orbits: drift of LAGEOS-2 perigee with respect to ecliptical longitude (309 days), draconitic year of LAGEOS-2 (222 days), LAGEOS-2 orbital alias with P_1 tide (138 days). Thus, the intention of a proper combination has been achieved, because the LAGEOS-based scale, which is much more stable, definitely dominates the LAGEOS + GNSS combination.

Summary and conclusions

The improvement in the ILRS network and the global geodetic parameters is important in the context of SLR contribution to the global geodetic observing system component, which can be achieved by improving models of data reduction, using observations to various constellations or expanding the ground observing network (Otsubo et al. 2016).

This study evaluates the potential contribution of SLR observations to new GNSS systems for the realization of SLR-derived reference frame and deriving global geodetic parameters. Some SLR stations, such as Russian and Chinese stations, provide much more SLR observations to GNSS because their major objective is to support the GLONASS and BeiDou constellations. The ILRS conducted a series of intensive campaigns of SLR tracking to GNSS satellites, starting in 2014. As a result, the number of SLR observation to GNSS exceeded the number of SLR observations to LAGEOS in the beginning of 2017 which allows employing GNSS observations for the ITRF realization. Moreover, the GNSS satellites, as opposed to Etalons, are active spacecraft; thus, their orbits can be fixed to microwave-based values or simultaneously processed on the basis of SLR-GNSS and microwave-GNSS data.

The solutions based only on SLR-to-GNSS data provide ERPs with the RMS of pole coordinates at the level of 400–500 µas and LOD with the RMS of 90 µas when fixing GNSS orbits. Re-substitution of annual range biases stabilizes the GNSS-only solutions when compared to the solution with estimating station-satellite-specific biases on the weekly basis. The combination of GNSS with LAGEOS data is especially beneficial for the LOD estimates and reduces the RMS of LOD by a factor of 3, whereas the pole coordinates assume similar quality to those based on LAGEOS data.

Geocenter coordinates based on SLR-to-GNSS data with estimating GNSS orbits when all GLONASS and only 3–4 Galileo satellites were active are of inferior quality. However, along with a progressive populating of Galileo orbital planes, the quality of geocenter components has been improved to the level better than 6 and 15 mm for equatorial and polar geocenter components, respectively. The scale of the reference frame and the geocenter coordinates in the combined LAGEOS + GNSS solutions are dominated by the LAGEOS data.

Using SLR observations to GNSS increases the number of weekly station coordinate solutions possible to obtain when compared to LAGEOS-only solution. The number of estimated station coordinates is 3909, 3476, and 4170 in LAGEOS-only, in GNSS-only, and in LAGEOS + GNSS, respectively when summing up all stations present in 7-day solutions in the period 2014.0–2017.4. This means that on average, 22, 20, and 24 stations contributed to 7-day LAGEOS-only, GNSS-only, and LAGEOS+GNSS solutions, respectively. Some stations provide by far more observations to GNSS than to LAGEOS, e.g., for Altay the number

Sośnica *et al. Earth, Planets and Space*   (2019) 71:20

Page 10 of 11

of solutions increased by 22%, for Komsomolsk by 41%, for Arkhyz by 39%, and for Brasilia by 30%. Moreover, when using range observations to GNSS in the solutions, station coordinate repeatability is improved for those stations that do not provide a lot of LAGEOS data or the range bias is estimated to LAGEOS (see Wettzell in Fig. 7) because the GNSS observations help to decorrelate the estimated range biases and the vertical components of station coordinates. We conclude that the future ITRF realizations should consider SLR observations to GNSS satellites in addition to the LAGEOS and Etalon observations.

As a next step, we will evaluate the full potential of ITRF realizations based on combined SLR observations to LAGEOS, LARES, and Etalon satellites, active low orbiting satellites, such as Sentinel-3A and Jason-3, and multi-constellation GNSS tracked by SLR.

Abbreviations

SLR: satellite laser ranging; GNSS: global navigation satellite system; CODE: Center for Orbit Determination in Europe; ECOM: Empirical CODE Orbit Model; EPRs: Earth rotation parameters; LOD: length of day; UTC: universal time; ITRF: International Terrestrial Reference Frame; IERS: International Earth Rotation and Reference System Service; LAGEOS: Laser Geodynamic Satellite; QZSS: Quasi-Zenith Satellite System; RMS: root mean square error; MEO: medium Earth orbit; IGSO: inclined geosynchronous orbit; ILRS: International Laser Ranging Service; IGS: International GNSS Service; MGEX: Multi-GNSS Experiment; NEQ: normal equation system; IOV: in-orbit validation; FOC: fully operational capability; PRN: pseudorandom noise satellite number; VLBI: very long baseline interferometry; DORIS: Doppler Orbitography Radiopositioning Integrated by Satellite.

Authors' contributions

KS, GB, and RZ performed GNSS computations. MD provided LAGEOS solutions. All authors have contributed to the interpretation of the results and the preparation of the manuscript. KS coordinated all activities. All authors read and approved the final manuscript.

Competing interests

The authors declare that they have no competing interests.

Availability of data and materials

SLR observations are provided by the https://ilrs.cddis.eosdis.nasa.gov/data_and_products/data/index.html CODE MGEX orbits are available from: http://ftp.aiub.unibe.ch/CODE_MGEX/CODE/ IERS-14-C04 series are available from: https://www.iers.org/IERS/EN/DataProducts/EarthOrientationData/eop.html SLRF2014 is available at: ftp://cddis.nasa.gov/slr/products/resource.

Consent for publication

Not applicable.

Ethics approval and consent to participate

Not applicable.

Publisher's Note

Springer Nature remains neutral with regard to jurisdictional claims in published maps and institutional affiliations.

References

Altamimi Z, Rebischung P, Metivier L, Collilieux X (2016) ITRF2014: a new release of the International Terrestrial Reference Frame modeling non-linear station motions. J Geophys Res Solid Earth 121:6109–6131. https://doi.org/10.1002/2016JB013098

Appleby GM (1998) Long-arc analyses of SLR observations of the Etalon geodetic satellites. J Geod 72(6):333–342. https://doi.org/10.1007/s001900050172

Appleby GM, Rodrguez J, Altamimi Z (2016) Assessment of the accuracy of global geodetic satellite laser ranging observations and estimated impact on ITRF scale: estimation of systematic errors in LAGEOS observations 1993–2014. J Geod 90(12):1371–1388. https://doi.org/10.1007/s00190-016-0929-2

Arnold D, Meindl M, Beutler G, Dach R, Schaer S, Lutz S, Prange L, Sośnica K, Mervart L, Jäggi A (2015) CODE's new solar radiation pressure model for GNSS orbit determination. J Geod 89(8):775–791. https://doi.org/10.1007/s00190-015-0814-4

Arnold D, Montenbruck O, Hackel S, Sośnica K (2018) Satellite laser ranging to low Earth orbiters: orbit and network validation. J Geod. https://doi.org/10.1007/s00190-018-1140-4

Bachmann S, Thaller D, Roggenbuck O, Lösler M, Messerschmitt L (2016) IVS contribution to ITRF2014. J Geod 90(7):631–654. https://doi.org/10.1007/s00190-016-0899-4

Bizouard C, Lambert S, Gattano C, Becker O, Richard J-Y (2018) The IERS EOP 14C04 solution for Earth orientation parameters consistent with ITRF 2014. J Geod. https://doi.org/10.1007/s00190-018-1186-3

Bloßfeld M, Gerstl M, Hugentobler U, Angermann D, Müller H (2014) Systematic effects in LOD from SLR observations. Adv Space Res 54:1049–1063. https://doi.org/10.1016/j.asr.2014.06.009

Bloßfeld M, Müller H, Gerstl M, Štefka V, Bouman J, Göttl F, Horwath M (2015) Second-degree Stokes coefficients from multi-satellite SLR. J Geod 89(9):857–871. https://doi.org/10.1007/s00190-015-0819-z

Bloßfeld M, Rudenko S, Kehm A, Panadina N, Müller H, Angermann D, Hugentobler U, Seitz M (2018) Consistent estimation of geodetic parameters from SLR satellite constellation measurements. J Geod. https://doi.org/10.1007/s00190-018-1166-7

Bruni S, Rebischung P, Zerbini S, Altamimi Z, Errico M, Santi E (2018) Assessment of the possible contribution of space ties on-board GNSS satellites to the terrestrial reference frame. J Geod. https://doi.org/10.1007/s00190-017-1069-z

Bury G, Sośnica K, Zajdel R (2018) Multi-GNSS orbit determination using satellite laser ranging. J Geod. https://doi.org/10.1007/s00190-018-1143-1

Bury G, Sośnica K, Zajdel R (2019) Impact of the atmospheric non-tidal pressure loading on global geodetic parameters based on satellite laser ranging to GNSS. IEEE Trans Geosci Remote Sens. https://doi.org/10.1109/TGRS.2018.2885845

Ciufolini I, Pavlis EC (2004) A confirmation of the general relativistic prediction of the Lense–Thirring effect. Nature 431(7011):958–960. https://doi.org/10.1038/nature03007

Cheng M, Ries J (2017) The unexpected signal in GRACE estimates of C20. J Geod 97(8):897–914. https://doi.org/10.1007/s00190-016-0995-5

Cox C, Chao B (2002) Detection of a large scale mass redistribution in the terrestrial system since 1998. Science 297:831–833

Dach R, Lutz S, Walser P, Fridez P (eds) (2015) Bernese GNSS Software Version 5.2. User manual. Astronomical Institute, University of Bern, Bern Open Publishing. https://doi.org/10.7892/boris.72297

Dach R, Susnik A, Grahsl A, Villiger A, Arnold D, Prange L, Schaer S, Jaggi A (2017) GLONASS satellite orbit modelling. In: Proceedings of the IGS workshop, Paris, pp 3–7. http://www.igs.org/assets/pdf/W2017-PY08-03%20-%20Dach.pdf

Dow J, Neilan R, Rizos C (2009) The international GNSS service in a changing landscape of global navigation satellite systems. J Geod 83(34):191–198. https://doi.org/10.1007/s00190-008-0300-3

Exertier P, Belli A, Samain E, Meng W, Zhang H, Tang K, Sun X (2018) Time and laser ranging: a window of opportunity for geodesy, navigation, and metrology. J Geod. https://doi.org/10.1007/s00190-018-1173-8

Fritsche M, Sośnica K, Rodriguez-Solano C, Steigenberger P, Dietrich R, Dach R, Wang K, Hugentobler U, Rothacher M (2014) Homogeneous reprocessing of GPS, GLONASS and SLR observations. J Geod 88(7):625–642. https://doi.org/10.1007/s00190-014-0710-3

Glaser S, Fritsche M, Sośnica K, Rodriguez-Solano C, Wang K, Dach R, Hugentobler U, Rothacher M, Dietrich R (2015) A consistent combination of GNSS and SLR with minimum constraints. J Geod 89(12):1165–1180. https://doi.org/10.1007/s00190-015-0842-0

Kucharski D, Kirchner G, Bennett JC, Lachut M, Sośnica K, Koshkin N, Suchodolski T (2017) Photon pressure force on space debris TOPEX/Poseidon measured by satellite laser ranging. Earth Space Sci 4:661668. https://doi.org/10.1002/2017EA000329

Lutz S, Steigenberger P, Meindl M, Beutler G, Sośnica K, Schaer S, Dach R, Arnold D, Thaller D, Jäggi A (2016) Impact of the arclength on GNSS analysis results. J Geod 90(4):365–378. https://doi.org/10.1007/s00190-015-0878-1

Lyard F, Lefevre F, Letellier T, Francis O (2006) Modelling the global ocean tides: modern insights from FES2004. Ocean Dyn 56:394415. https://doi.org/10.1007/s10236-006-0086-x

Mendes VB, Pavlis EC (2004) High-accuracy zenith delay prediction at optical wavelengths. Geophys Res Lett 31:L14602. https://doi.org/10.1029/2004GL020308

Meng W, Zhang H, Zhang Z, Prochazka I (2013) The application of single photon detector technique in laser time transfer for Chinese navigation satellites. In: Photon counting applications IV; and quantum optics and quantum information transfer and processing, vol 8773, p 87730E

Montenbruck O, Steigenberger P, Prange L, Deng C, Zhao Q, Perosanz F, Romero I, Noll C, Sturze A, Weber G, Schmid R, MacLeod K, Schaer S (2017) The multi-GNSS experiment (MGEX) of the International GNSS Service (IGS) achievements, prospects and challenges. Adv Space Res 59(7):1671–1697. https://doi.org/10.1016/j.asr.2017.01.011

Otsubo T, Appleby G (2003) System dependent center of mass correction for spherical geodetic satellites. J Geophys Res 108(2201):B4. https://doi.org/10.1029/2002JB002209

Otsubo T, Appleby G, Gibbs P (2001) GLONASS laser ranging accuracy with satellite signature effect. SGEO 22(56):509–516. https://doi.org/10.1023/A:1015676419548

Otsubo T, Matsuo K, Aoyama Y, Yamamoto K, Hobiger T, Kubo-oka T, Sekido M (2016) Effective expansion of satellite laser ranging network to improve global geodetic parameters. Earth Planets Space 68(1):65. https://doi.org/10.1186/s40623-016-0447-8

Pardini C, Anselmo L, Lucchesi DM, Peron R (2017) On the secular decay of the LARES semi-major axis. Acta Astronaut 140:469–477

Pavlis EC (1994) High resolution Earth orientation parameters from LAGEOS SLR data analysis at GSFC, in IERS Technical Note 16

Pavlis NK, Holmes SA, Kenyon SC, Factor JK (2013) Erratum: Correction to the development and evaluation of the earth gravitational model 2008 (EGM2008). J Geophys Res Solid Earth 118:2633. https://doi.org/10.1002/jgrb.50167

Pearlman M, Degnan J, Bosworth J (2002) The international laser ranging service. Adv Space Res 30(2):135–143. https://doi.org/10.1016/S0273-1177(02)00277-6

Pearlman M, Arnold D, Davis M, Barlier F, Biancale R, Vasiliev V, Ciufolini I, Paolozzi A, Pavlis E, Sośnica K, Bloßfeld M (2019) Laser geodetic satellites: a high accuracy scientific tool. J Geod. https://doi.org/10.1007/s00190-019-01228-y

Petit G, Luzum B (2010) IERS Conventions (2010). IERS Technical Note 36. Verlag des Bundesamts fuer Kartographie und Geodaesie, Frankfurt am Main, ISBN 3-89888-989-6

Prange L, Orliac E, Dach R, Arnold D, Beutler G, Schaer S, Jäggi A (2017) CODE's five-system orbit and clock solution the challenges of multi-GNSS data analysis. J Geod 91(4):345–360. https://doi.org/10.1007/s00190-016-0968-8

Sośnica K, Jäggi A, Thaller D, Dach R, Beutler G (2014) Contribution of Starlette Stella and AJISAI to the SLR-derived global reference frame. J Geod 88(8):789–804. https://doi.org/10.1007/s00190-014-0722-z

Sośnica K, Jäggi A, Meyer U, Thaller D, Beutler G, Arnold D, Dach R (2015a) Time variable Earth's gravity field from SLR satellites. J Geod 89(10):945–960. https://doi.org/10.1007/s00190-015-0825-1

Sośnica K, Thaller D, Dach R, Steigenberger P, Beutler G, Arnold D, Jäggi A (2015b) Satellite laser ranging to GPS and GLONASS. J Geod 89(7):725–743. https://doi.org/10.1007/s00190-015-0810-8

Sośnica K, Bury G, Zajdel R (2018a) Contribution of multi-GNSS constellation to SLR-derived terrestrial reference frame. Geophys Res Lett 45:2339–2348. https://doi.org/10.1002/2017GL076850J

Sośnica K, Prange L, Kaźmierski K, Bury G, Drożdżewski M, Zajdel R, Hadaś T (2018b) Validation of Galileo orbits using SLR with a focus on satellites launched into incorrect orbital plane. J Geod 92(2):131–148. https://doi.org/10.1007/s00190-017-1050-x

Strugarek D, Sośnica K, Jäggi A (2019) Characteristics of GOCE orbits based on satellite laser ranging. Adv Space Res 63(1):417–431. https://doi.org/10.1016/j.asr.2018.08.033

Thaller D, Sośnica K, Dach R, Beutler G, Mareyen M, Richter B (2014) Geocenter coordinates from GNSS and combined GNSS–SLR solutions using satellite co-locations. In: International association of geodesy symposia, vol 139. Springer, Berlin, pp 129-134. https://doi.org/10.1007/978-3-642-37222-3_16

Thaller D, Sośnica K, Steigenberger P, Roggenbuck O, Dach R (2015) Pre-combined GNSS–SLR solutions: what could be the benefit for the ITRF? In: International association of geodesy symposia, vol 146. Springer, Berlin, pp 85–94. https://doi.org/10.1007/1345_2015_215

Zajdel R, Sośnica K, Bury G (2017) A new online service for the validation of multi-GNSS orbits using SLR. Remote Sens 9:1049. https://doi.org/10.3390/rs9101049